SAND2012-0766C

High precision fabrication of polarization insensitive resonant grating filters

R. R. Boye, D.W. Peters, J.R. Wendt, S. Samora, J. Stevens, R.J. Shul, J. Hunker, R.A. Kellogg and S.A. Kemme

Sandia National Laboratories, Albuquerque, NM 87185

ABSTRACT

Resonant subwavelength gratings have been designed and fabricated as wavelength-specific reflectors for application as a rotary position encoder utilizing ebeam based photolithography. The first grating design used a two-dimensional layout to provide polarization insensitivity with separate layers for the grating and waveguide. The resulting devices had excellent pattern fidelity and the resonance peaks and widths closely matched the expected results. Unfortunately, the gratings were particularly angle sensitive and etch depth errors led to shifts in the center wavelength of the resonances. A second design iteration resulted in a double grating period to reduce the angle sensitivity as well as different materials and geometry; the grating and waveguide being the same layer. The inclusion of etch stop layers provided more accurate etch depths; however, the tolerance to changes in the grating duty cycle was much tighter. Results from these devices show the effects of small errors in the pattern fidelity. The fabrication process flows for both iterations of devices will be reviewed as well as the performance of the fabricated devices. A discussion of the relative merits of the various design choices provides insight into the importance of fabrication considerations during the design stage.

Keywords: Subwavelength, diffractive optical element, resonant grating, guided mode resonance filter

INTRODUCTION

Resonant subwavelength gratings (RSG), also known as guided mode resonance filters, take advantage of the interaction of a diffracted order from a grating and a waveguide mode.[1, 2] This interaction leads to a resonance behavior that can provide excellent devices for filtering applications. Typically, the grating period is set to a value that has only one propagating order in the higher index of the waveguide to avoid losses to other orders. Designs use a wavelength and incidence angle that overlaps this propagating order with an allowed mode of a slab waveguide adjacent to the grating. By also designing the device to have a low reflection at the same wavelength[3], sharp transitions from very low reflection to very high can be fabricated. Devices with extremely high efficiency[4] have been demonstrated as well as devices with both extremely narrow and wider resonance peaks[5].

In this paper, we present the fabrication of two RSG designs for a rotary position encoder.[6] The RSGs are intended to act as wavelength specific reflectors with a different wavelength used to encode different bits on a position encoder disc. The system was designed to be interrogated via fiber using wavelengths available from a tunable telecommunications laser. The first grating design used titanium dioxide (TiO_2) for both the waveguide and grating. Despite inherent limits on the accuracy of a timed etch, these gratings provided excellent resonant responses and a successful application demonstration. A second iteration using a silicon based design was intended to provide some advantages including better etch depth accuracy. Unfortunately, the choice of a single waveguide/grating layer utilizing a silicon/air grating led to unintended fabrication tolerances. A short description of the application and its requirements is provided in the next section to provide the context for the grating designs. The design, fabrication and testing of each design iteration is then provided. Finally, conclusions from this work as well as improvements to be made in subsequent development are given.

ENCODER APPLICATION AND REQUIREMENTS

One of the main advantages of an all optical encoder is the elimination of all electrical connections and electrical components. In addition, minimizing the number of fiber connections reduces the number of openings in the package containing the encoder resulting in a corresponding reduction in packaging complexity. To take advantage of this, the conceptual design for the encoder assumed a single fiber ferrule used to illuminate the encoder and receive the reflected optical signal. The device would then consist of only the encoder, fiber and collimating optic with the source and detection electronics located remotely and connected via the fiber.

The basic approach for the optical readout of the encoder is shown in Figure 1. For this project, it was assumed that each bit required would correspond to a wavelength and would require an RSG with the matching resonance. Four bits were implemented here allowing for the determination of sixteen positions around the encoder. In the time-gated approach implemented, the individual bits are read sequentially with the illumination provided by a single tunable source. Since only one bit is read at a time, only a single detector is needed and there is no need for a demultiplexing component on the return signal; allowing for the use of a multimode fiber to receive the reflected signal. In addition, the use of telecommunications wavelengths was chosen because of the availability of components, including the tunable laser, in this spectral region.

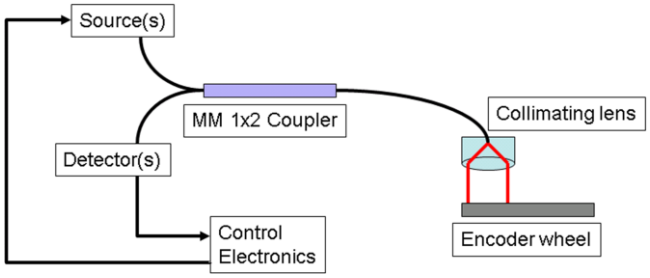

Figure 1. Basic schematic approach for optical readout of encoder with wavelength multiplexed bits.

The requirements for the individual RSGs and their layout on the encoder disc were driven by the conceptual framework for the encoder implementation. RSG designs would be needed for each bit and each position mark would be segregated spatially into the four bits. If a bit needed to be high in a particular position, the RSG would be present; otherwise, an effective anti-reflection grating would take its place. The wavelength spacing of the resonances was chosen so that all of the bits could be addressed by the tunable laser, a LambdaFLEX™ iTLA from Bookham, having a range of 1528-1563 nm. The RSG designs also needed to have a wide enough full width (FWHM) to accommodate fabrication and alignment tolerances. To avoid the use of polarization maintaining fiber, the RSGs needed to be polarization insensitive.

The actual layout of the encoder disc is shown in Figure 2. The position marks were made fairly small, 1.2 mm on a side, to ensure good positional accuracy and to match the collimated output from the input fiber using a lens with a moderately short focal length lens (approximately 7 mm). To help ensure the position of the encoder with respect to the input beam, a fifth "check" bit grating was added to the position marks.

ORIGINAL DESIGN WITH TITANIUM DIOXIDE

The first grating design utilized TiO_2 for the waveguide and grating with a two-dimensional geometry for polarization insensitivity.[7] The analysis and design of the two dimensional RSGs was done using rigorous coupled wave analysis (RCWA).[8-10] The geometry of the grating is shown in Figure 3. The substrate is silicon and was chosen for several reasons including excellent flatness and thin film adhesion, but the most important reason was the compatibility of silicon with deep reactive ion etch (DRIE) processes. The DRIE process was used to define the overall encoder part geometry. Its impact on the individual grating design was minimal (aside from the choice of substrate material) and will not be discussed in detail here. The silicon dioxide layer was designed to be as thin as possible while still acting as a cladding for the titanium dioxide

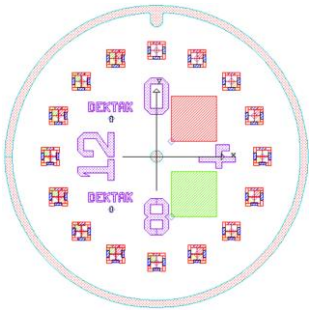

Figure 2. The layout of the encoder disc showing the sixteen position marks. The two large rectangles are test gratings for bits 1 and 4. The text is metal patterned in the same step as the wafer alignment marks (not shown).

waveguide layer. The TiO_2 thickness was set to provide a single mode slab waveguide for the design wavelength range. Finally, a top surface grating is etched directly into the TiO_2 to provide coupling between a diffracted mode and the propagating waveguide mode.

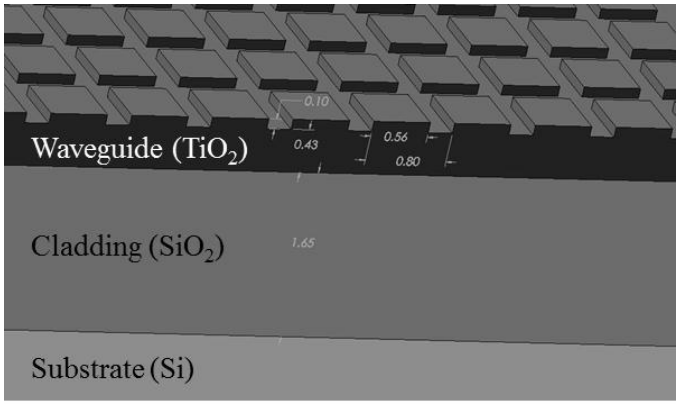

Figure 3. Geometry of two dimensional RSG. A thick layer of SiO_2 on top of the substrate acts as a cladding layer for the TiO_2 waveguide. A grating is etched into the top layer of the TiO_2.

To simplify the fabrication, the individual RSG designs were constrained to have the same grating depth, leaving the grating period as the free parameter used to properly locate the resonances. Additionally, the duty cycle for the pillars was set at 0.7 to make the structures polarization independent at or near normal incidence. The five grating periods were set at 786, 791, 795 and 799 nm for the four bits and 803 nm for a check bit. The grating depth was set at 100 nm with an underlying layer of 430 nm for the waveguide. The simulated resonances are shown in Figure 4 with peak wavelengths of 1532, 1539, 1546, 1553 and 1560 nm and FWHM of 2.5-2.6 nm. These wide resonances are due to the strength of the 100 nm deep TiO_2/air grating.

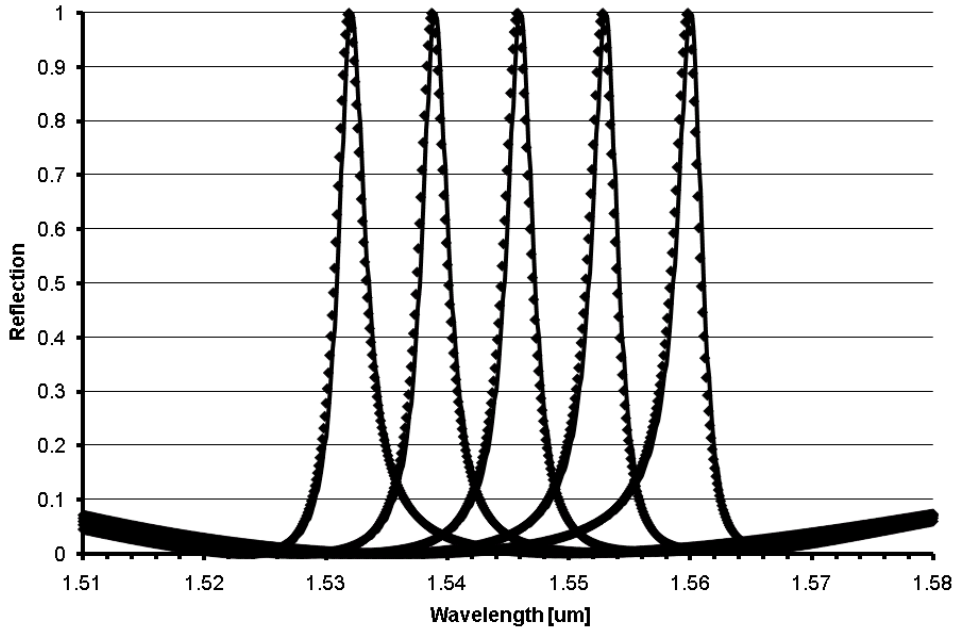

Figure 4. Plot of simulated responses of RSG devices with normally incident input. TE responses are shown with the solid lines while the individual marks represent the TM responses.

The strong interaction of the grating with the waveguide mode results in a short interaction length. This short interaction length allowed the grating size to be fairly small (600 nm) without impacting the resulting resonance peaks.[11-12]

The first step in the fabrication of the RSGs was the deposition of the thin film layers by a vendor. The received films were evaluated using SEM measurement of the film thicknesses and ellipsometry measurements of the indices. Measured thicknesses for the TiO_2 layer ranged from 507 – 550 nm (target = 530 nm) while the SiO_2 layer ranged from 1590 – 1680 nm (target = 1650 nm). Ellipsometry was done to check the refractive index of the layers, particularly the waveguide layer. The calculated index of the TiO_2 was found to be 2.205-2.216 at a wavelength of 1551 nm. These measurements were used to tune the grating periods slightly using RCWA to make sure the resonances were as close as possible to the desired wavelengths.

With the films in place, a reference metal layer was patterned to allow for alignment of subsequent patterning steps and provide visible markers to aid in testing and alignment. An adhesion layer of titanium, 10 nm thick, was followed by a 150 nm thick layer of gold. A standard liftoff process using 5214 photoresist was used to pattern the metal. The grating patterns were then written into ZEP using an e-beam write. The desired etch depth was 100 nm so the ZEP was thick enough to use as the etch mask. Test patterns were written to determine the proper dose. In addition, the CAD layout was biased to allow for characteristic widening of the written geometries. The grating etch was done using reactive ion etch (RIE) with a CHF_3/O_2 based chemistry. Without an etch stop layer, the grating etch had to be timed. A test etch immediately preceding the device etch was done to determine the proper duration. A SEM of the resulting two dimensional gratings is shown in Figure 5.

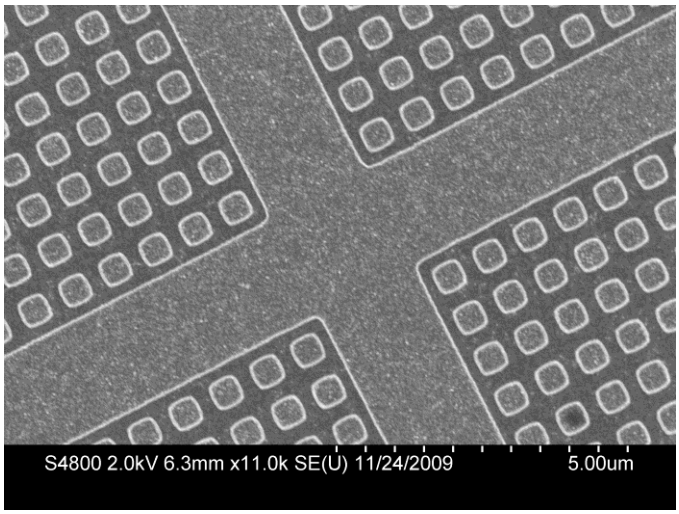

Figure 5. SEM image at the intersection of four RSG gratings in the middle of a single position mark on the encoder disc.

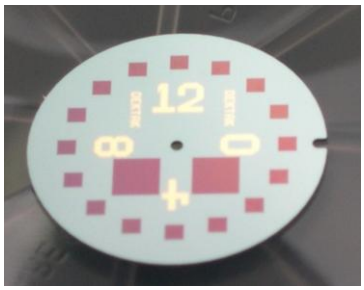

Figure 6. Completed encoder disc with two large test gratings and sixteen position marks comprised of several gratings.

To release the encoder disc from the larger wafer, a DRIE process was done. A thick photoresist layer was patterned and an initial RIE was performed to remove the TiO_2 first. Then the wafer was mounted on a carrier wafer and a DRIE was used to etch through the entire device wafer, releasing the encoder disc. Figure 6 shows the completed encoder disc.

ORIGINAL DEVICE TESTING

Fabricated RSG devices were first tested using single mode fiber to illuminate the disc and a bare detector to receive the reflected signal. The larger test gratings on the discs, see Figures 2 and 6, had bit 1 and 4 gratings. Measured results from these gratings are shown in Figure 7. It is clear that the measured resonance peaks are shifted from the

designed wavelengths. Possible reasons for this include an over-etched grating, a different refractive index than the assumed value and slightly off-axis incidence. The etch depth was checked by measuring a large test feature with a Dektak profilometer. The target depth for the test feature was set 10% beyond the target for the grating to account for loading effects in the small features. The measured etches were within 5% of this value; however, a rigorous measurement of the actual grating depth was not done since it would require a destructive SEM measurement. Additionally, errors in the index of the waveguide have a profound effect on the propagation vector of the waveguide mode and lead to substantial shifts of the resonance location. The range of indices found through ellipsometry can potentially cause a shift of as much as 7 nm.

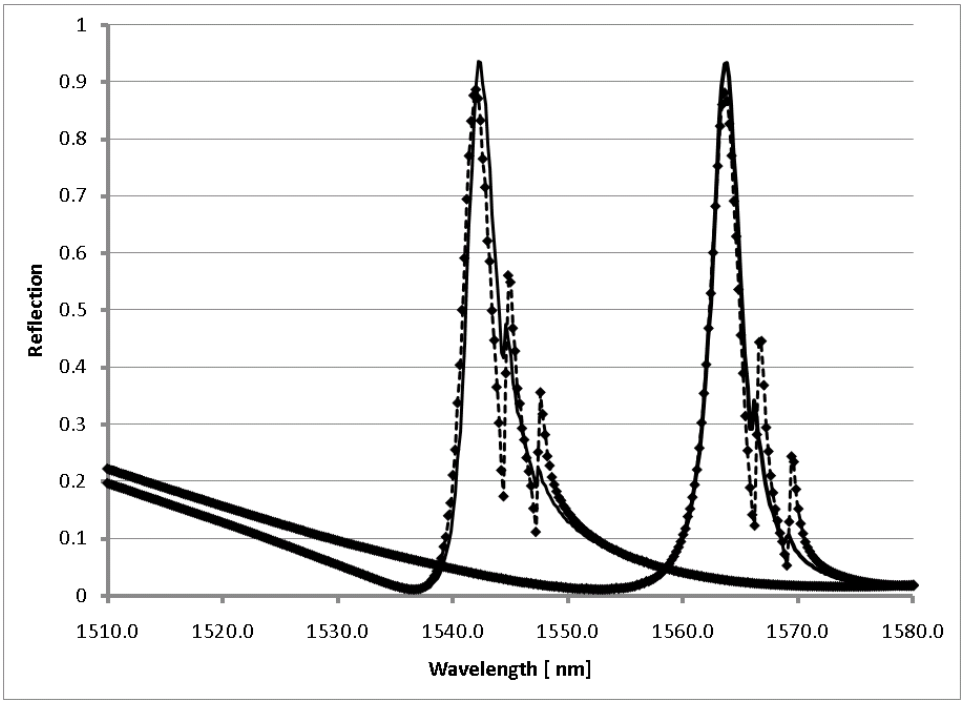

Figure 7. Measured responses of bits 1 and 4. TE responses shown with solid lines, TM with dotted lines and data marks.

An important result shown in Figure 7 is the polarization insensitivity. Plots for TE and TM incidence show a minimal shift of the resonance peaks as expected from the two dimensional grating. The peak response is excellent, > 93% for TE and > 88% for TM, and the FWHM has increased only marginally from the modeled results, 2.9-3.0 nm versus the 2.5-2.6 nm shown in Figure 4. Small losses in the material as well as slight nonuniformities across the larger test devices are the probable causes for these slight deviations from the simulated responses. Sidelobe peaks are visible on the long wavelength side for both measurements and are indicative of a small, non-zero angle of incidence.

Despite the shift of resonance peak locations, the encoder worked properly for all 64 bits (16 locations x 4 bits).[6] Figure 8 shows the hardware for the encoder demonstration including the optical interrogation of the encoder disc (left) as well as the laser and detector hardware (right). Figure 9 shows a screen shot from the program controlling the laser and displaying the bit states while the encoder was at position 13. The plot at the bottom of the screen shows the response of the laser at all 89 available channels. Notice that three resonance peaks are clearly visible while there is a gap where bit 2 is located.

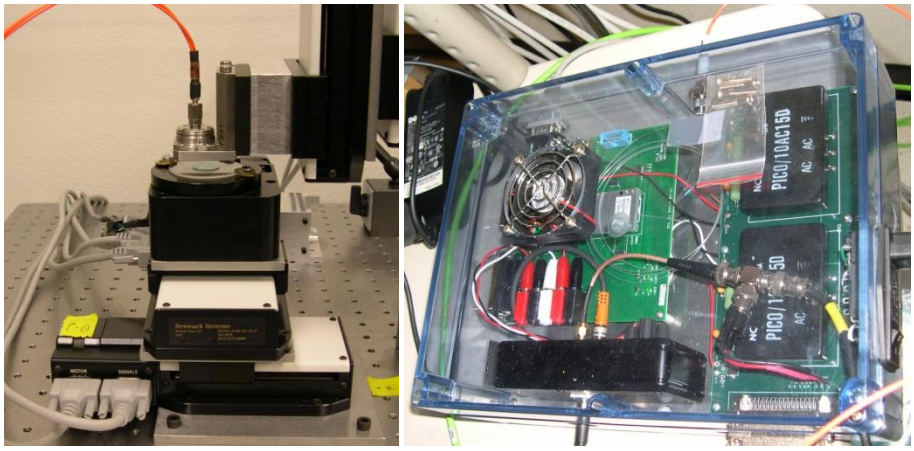

(a) *(b)*

Figure 8. (a) The encoder disc mounted on linear stages for initial alignment and a rotation stage for stepping between position marks. The dual fiber ferrule is mounted above the disc. (b) The tunable laser (under the cooling fan) and detector with preamplifier (black box at bottom) are packaged with power transformers. The input single mode fiber can be seen at the top of the figure while the return multimode fiber is connected to the detector at the bottom of the figure.

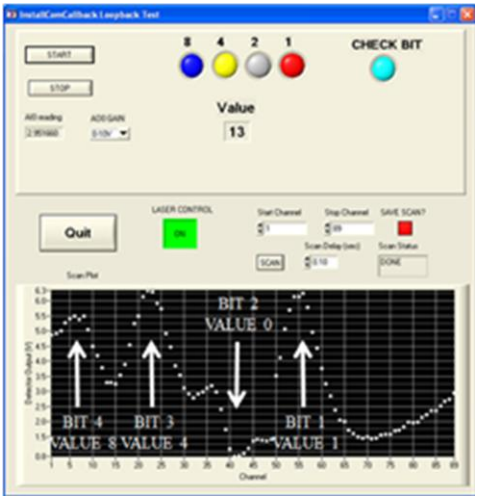

Figure 9. Screen shot of encoder program showing bits being properly read at position 13 as well as a scan of laser channels showing the three resonances corresponding to the three lighted bits.

SECOND DESIGN - SILICON

The successful laboratory demonstration of the encoder was followed by a second iteration intended to provide several improvements over the original. Some of these improvements did not impact the design of the resonant gratings. For instance, anti-reflection gratings were added between position marks to avoid spurious reflections when the encoder disc was moving between positions. In contrast, the grating design was changed to allow a wider tolerance for the incident angle on the input. Additionally, it was decided to pursue a design with an etch stop layer to better control the etch of the grating.

To address the need for a wider angular tolerance, a double grating was designed [13] and an existing etch process with high selectivity between silicon and SiO_2 was chosen to enable the fabrication. The double period grating geometry is shown in Figure 10. The substrate is again silicon with a thick (2.65 μm) SiO_2 cladding layer. A layer of polysilicon, 200 nm thick, is patterned to provide both the grating and waveguide layer. The final material is a layer of SiO_2 which acted as the masking layer during the silicon etch. Using the same grating depth, five grating periods, 1042, 1045, 1048, 1051 and 1054 nm, were determined for providing resonances in the same wavelength region as the original design. The gaps were kept constant at 130 and 260 nm with the pillar widths varying. The simulated response of these gratings is shown in Figure 11.

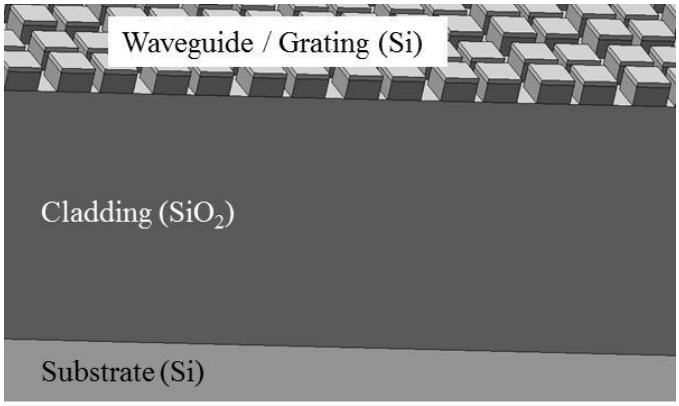

Figure 10. Geometry of two dimensional RSG with double grating. A thick layer of SiO_2 (2.65 μm) on top of the substrate acts as a cladding layer for the Si waveguide/grating (200 nm). The top layer of SiO_2 was used as the etch mask during the silicon etch process. The gaps were 130 and 260 nm with the period ranging from 1.042 to 1.054 μm.

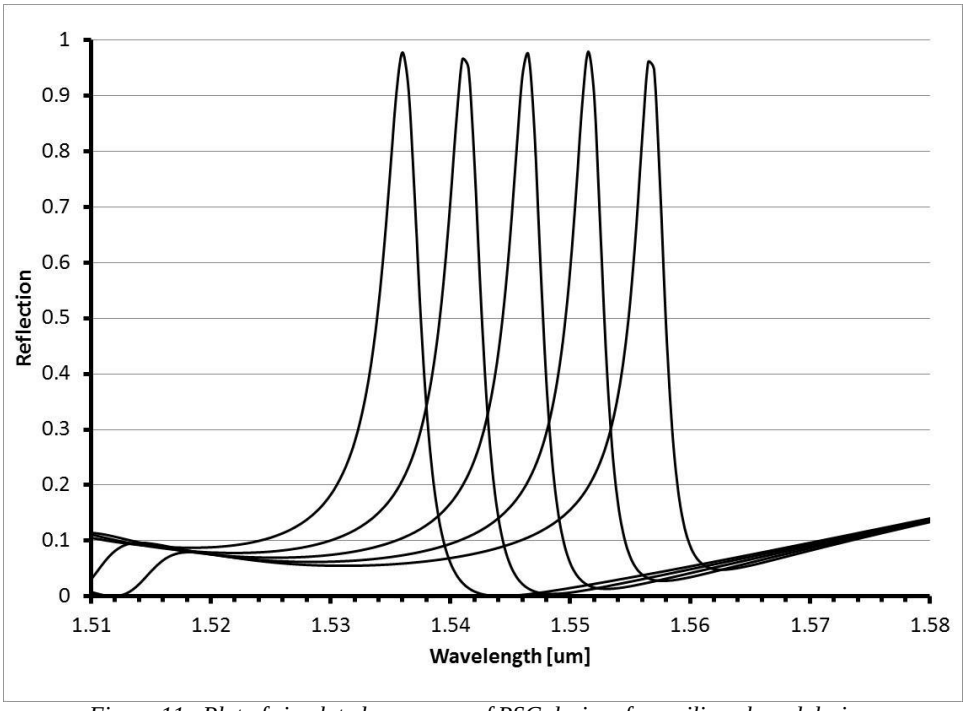

Figure 11. Plot of simulated responses of RSG devices from silicon based design.

The fabrication of these devices began with the thermal oxidation of the silicon wafers providing the thick SiO_2 layer required by the design. Using the thermal oxide avoided problems with stresses from a thick film on one side of the wafer and provided excellent uniformity across the wafer. Several test wafers were included during the deposition processes so the actual thicknesses and refractive indices could be measured via ellipsometry and the design geometry appropriately tailored before the photolithography. The resulting thickness for the oxide growth was found to be within 0.5% of the specified design thickness with a refractive index ranging from 1.4468 (λ = 1.45 mm) to 1.4443 (λ = 1.65mm). The waveguide/grating layer was polysilicon deposited by chemical vapor deposition followed by the final SiO_2 deposition of 100 nm. The measured silicon layer was 200.9 nm thick with indices ranging from 3.7848 (λ = 1.45 mm) to 3.7588 (λ = 1.65mm).

The same metal liftoff process described earlier was used to put down reference marks for alignment of the remaining process steps. The subsequent e-beam lithography was modified from the previous design. The ZEP photoresist used previously was replaced with the more common PMMA. There were two main reasons for this change. First, the top oxide layer would be patterned first as a hard etch mask for the silicon etch so the resist only had to withstand the first, shorter etch. Second, the smallest features to be patterned were 100 nm, considerably smaller than the previous design. There was a third reason – cost. The first fabrication iteration was done with 2" diameter wafers. The silicon based design was fabricated on 6" wafers requiring significantly more photoresist. Similar to the previous devices, the geometric layout was biased and several doses were tested to ensure excellent pattern fidelity.

The etching of the waveguide/grating was done in two steps. First, a conventional oxide etch using a 100% CHF_3 chemistry was done. This etch does not have particularly high selectivity between the oxide and silicon so endpoint detection was done to terminate the etch at the proper time. (It should be noted that an over-etch at this point in the process would not cause subsequent problems in the remaining process steps.) Next, a HBr/Ar based etch was used to etch the silicon, again using endpoint detection to terminate at the proper time. The selectivity between silicon and SiO_2 etch rate is between 6:1 and 7:1, providing excellent control of the etch depth. The final fabricated grating had a residual oxide layer of approximately 30 nm on top of the silicon pillars. A SEM image of the final grating is shown in Figure 12.

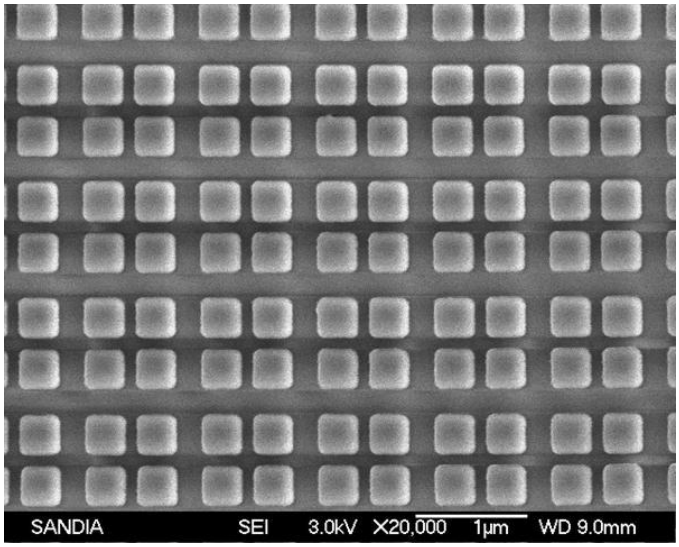

Figure 12. SEM image of double period silicon waveguide grating.

Once the devices were fabricated, a missing element in the process flow was uncovered. While the design and process were designed to provide excellent etch depth control and lithography pattern fidelity, the duty cycle of the grating was adversely affected by an effective bias during the etch. This was not a concern for the original design where the waveguide and grating were different layers. A change in duty cycle in that device would have only a marginal effect on the resulting resonance peak location with the larger effect being a change in the width of the peak. For this device, where the grating was also the waveguide, the effective index of the layer would change rapidly with duty cycle due to the large difference in index between the air and silicon. This would, in turn, lead to a significant change in the propagation vector in the waveguide, completely changing the resonance condition. Subsequent testing of the gratings verified the deleterious effects of this oversight.

Using the same test apparatus described earlier, tests on the double period, silicon gratings resulted in poor responses. An example of a measured response is shown in Figure 13 along with a simulated result using the measured geometric parameters of the fabricated gratings. The loss in peak response can be attributed to the geometric deviation from design parameters as shown by the simulated response. Additionally, the peak is wider than expected with higher reflection away from the peak. Part of this is due to measurement error, but other sources of scattering in the fabricated parts may

be contributing as well. One possible source is the polysilicon layer. Its amorphous structure can contain crystallites formed during heating of subsequent processing steps such as the top oxide deposition or etching.

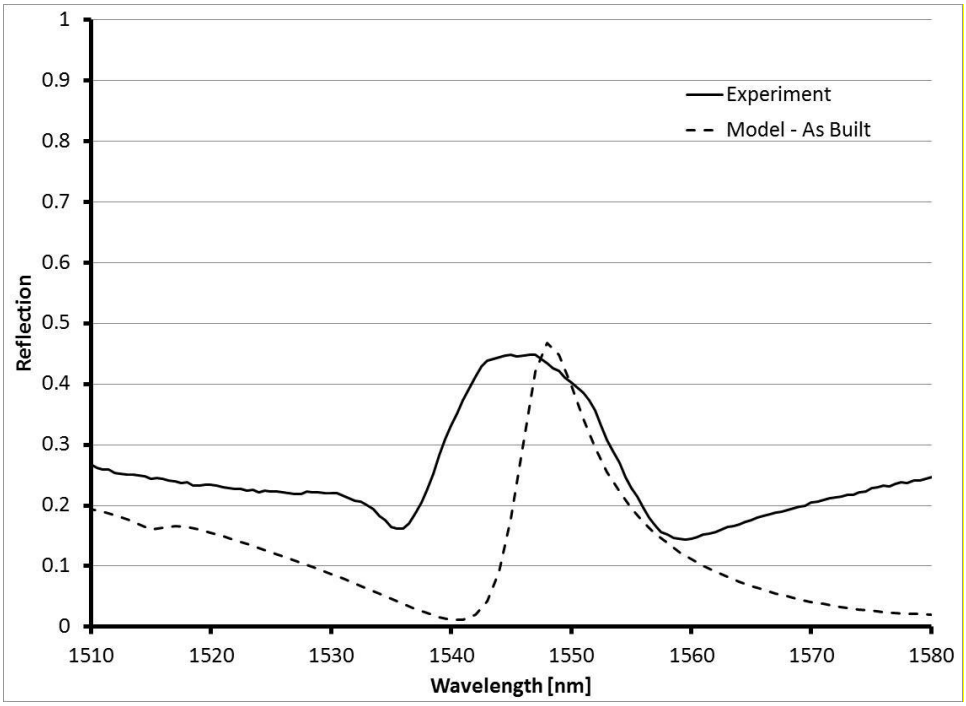

Figure 13. Data and simulation of the silicon grating response.

Clearly, the performance of these gratings is inferior to the original design. The change in feature size caused by the etch process was as large as 30 nm. The use of the silicon waveguide grating resulted in extremely tight tolerances for the grating duty cycle and fabricated devices not suitable for the end application.

ANALYSIS AND CONCLUSIONS

The original goal of this program was the successful application of RSGs to a rotary position encoder. This goal was met using a TiO_2 based RSG design; however, an attempt at an improved system was not successful due to design choices that ultimately led to unrecognized fabrication constraints. Simulated results of the silicon based designs did show an increase in angular tolerance; however, the use of a silicon/air grating as the waveguide led to very tight tolerances on the duty cycle of the grating. Fabricated gratings did not meet this tolerance and the resulting device responses were poor. The missing element in the design and processing was the accommodation of the bias due to the etching process. It may be possible to characterize this bias sufficiently or to run test structures that take into account biases from the e-beam lithography and the etching in order to pre-bias the design. Of course, the design process should also include a determination of the magnitude of this tolerance, particularly when it affects the waveguide layer.

In hindsight, a more successful design path would probably have kept the grating and waveguide layers separate (or at least not use such a high index material with air). The TiO_2 design was easily modified to include a double grating to provide the improved angular resonance. This design wasn't used because of the desire to include an etch stop layer. Readily available materials and processes did not provide a straightforward development path using TiO_2.

While this program provided a successful solution for a demonstration, it would be helpful to further improve it to make it viable in a real world environment. The first attempt at such improvements resulted in important lessons in understanding the dependencies of RSG designs and the impact of fabrication capabilities. Future iterations of this

project will incorporate designs based on the original structure and may include development of etch processes that provide more convenient etch stop options.

ACKNOWLEDGMENTS

Sandia National Laboratories is a multi-program laboratory managed and operated by Sandia Corporation, a wholly owned subsidiary of Lockheed Martin Corporation, for the U.S. Department of Energy's National Nuclear Security Administration under contract DE-AC04-94AL85000.

REFERENCES

[1] Wang, S.S., Magnusson, R., Bagby, J.S. and Moaharam, M.G., "Guided-mode resonances in planar dielectric-layer diffraction gratings," JOSA A, 7(8), 1470-1474 (1990).
[2] Avrutskii, I.A. and Sychugov, V.A., "Reflection of a Gaussian light beam from the surface of a corrugated waveguide," Sov. J. Quant. Electron., 16(11), 1558-1559 (1986).
[3] Magnusson, R., Shin, D. and Liu, Z.S., "Guided-mode resonance Brewster filter," Opt. Lett., 23(8), 612-614 (1998).
[4] Liu, Z.S., Tibuleac, S., Shin, D., Young, P.P. and Magnusson, R., "High-efficiency guided-mode resonance filter," Opt. Lett., 23(19), 1556-1558 (1998).
[5] Brundrett, D.L., Glytsis, E.N. and Gaylord, T.K., "Normal-incidence guided-mode resonant grating filters: design and experimental demonstration," Opt. Lett., 23(9), 700-702 (1998).
[6] Boye, R.R., Peters, D.W., Wendt, J.R., Shul, R.J., Samora, S., Rich, S.G., Carter, T., Lentine, A.L., Kellogg, R.A. and Kemme, S.A., "Applicatioin of resonant subwavelength gratings to a rotary position encoder," Proc. SPIE, 7604, 76040P1-76040P9 (2010).
[7] Peters, D.W., Boye, R.R., Wendt, J.R., Kellogg, R.A., Kemme, S.A., Carter, T.R., Samora, S., "Demonstration of polarization-independent resonant subwavelength grating filter arrays," Opt. Lett., 35(19), 3201-3203 (2010).
[8] Moharam, M.G., Grann, E.B., Pommet, D.A. and Gaylord, T.K., "Formulation for stable and efficient implementation of the rigorous coupled-wave analysis of binary gratings," JOSA A, 12(5), 1068-1076 (1995).
[9] Moharam, M.G., Grann, E.B., Pommet, D.A. and Gaylord, T.K., "Stable implementation of the rigorous coupled-wave analysis for surface relief gratings: enhanced transmittance matrix approach," JOSA A, 12(5), 1077-1086 (1995).
[10] Lalanne, P. and Morris, G.M., "Highly improved convergence of the coupled-wave method for TM polarization," JOSA A, 13(4), 779-784 (1996).
[11] Boye, R.R. and Kostuk R.K., "Investigation of the effect of finite grating size on the performance of guided mode resonance filters," Appl. Opt., 39(21), 3649-3653 (2000).
[12] Peters, D.W., Kemme, S.A. and Hadley, G.R., "Effect of finite grating, waveguide width, and end-facet geometry on resonant subwavelength grating reflectivity," JOSA A, 21(6), 981-987 (2004).
[13] Fehremback, A-L., Talneau, A., Boyko, O., Lemarchand, F. and Sentenac, A., "Experimental demonstration of a narrowband, angular tolerant, polarization independent, doubly periodic resonant grating filter," Opt. Lett., 32(15), 2269-2271 (2007).